Diagrammatic Design of Ansätze for Quantum Chemistry

Ayman El Amrani

St. John's College

A thesis submitted for the Honour School of Chemistry

Part II 2024

Pour ma mère et mon père.

Summary

A central challenge in computational quantum chemistry is the accurate simulation of fermionic systems. At the heart of these calculations lies the need to solve the Schrödinger equation to determine the many-electron wavefunction. An exact solution to this problem scales exponentially with the number of electrons. Classical computers struggle to store the increasingly large wavefunctions making this problem computationally intractable in many cases. In contrast, gate-based quantum computing presents a promising solution, offering the potential to represent electronic wavefunctions with polynomially scaling resources [1]. In other words, quantum computers are a natural tool of choice for simulating processes that are inherently quantum [2].

In the last two decades many advancements in quantum computing have been made in both hardware and software bringing us closer to being able to simulate molecular systems. Despite these advancements, we remain in the so-called Noisy Intermediate Scale Quantum (NISQ) era, characterised by challenges such as poor qubit fidelity, low qubit connectivity and limited coherence times. The NISQ era represents a transitional phase in quantum computing, where quantum devices are not yet error-corrected but are still capable of performing computations beyond the reach of classical computers. Overcoming the limitations of the NISQ era is crucial for realising the full potential of quantum computing in various fields, including quantum chemistry and materials science.

The Variational Quantum Eigensolver (VQE) algorithm is a method used to estimate the ground state energy of a molecular Hamiltonian by preparing a trial wavefunction,

calculating its energy, and optimising the wavefunction parameters classically until the energy converges to the best approximation for the ground state energy [3]. It is recognised as a leading algorithm for quantum simulation on NISQ devices due to its reduced resource requirements in terms of qubit count and coherence time [4].

This thesis extends methods developed by Richie Yeung [2] for the preparation and analysis of parametrised quantum circuits, and applies them to ansätze representing fermionic wavefunctions. We are concerned with two main questions on this theme. Firstly, can we use the ZX calculus [cite] to gain insights into the structure of the unitary product ansatz in the context of variational algorithms for quantum chemistry? Secondly, in the context of NISQ devices, can we use these insights to build better ansätze with reduced circuit depth and more efficient resources?

Contents

Appendices

Chapter 1

Background

In this chapter, we will discuss the framework that we use to simulate fermionic systems on a quantum computer, as well as the notation that we will use throughout the text. Starting with Quantum Computation REF(quantum-computation) and Electronic Structure Theory REF(electronic-structure-theory), we will build up to unitary coupled cluster theory and the Variational Quantum Eigensolver REF(vqe).

Fermionic states can generally be represented on a quantum computer in the occupation number representation (section REF(second-quantisation)). That is, the state of each qubit is taken to represent the occupancy of each spin orbital. By representing the fermionic creation and annhilation operators in terms of qubit operators in a way that preserves the fermionic anticommutation relations, we can express the molecular Hamiltonian in terms of qubit operations.

1.1 Quantum Computation

Introduction to Qubits

In contrast to classical computation, where bits form the basis for encoding information, quantum computation makes use of quantum bits (qubits). There are many physical implementations of qubits, however, for the purposes of this thesis, it will suffice to think of them as purely mathematical objects.

Qubits can exist as superpositions of the computational basis: the $|0\rangle$ and $|1\rangle$ states. These states are orthonormal vectors in a two-dimensional complex Hilbert space $\mathbb{C}^2$. We can depict these states on a Bloch sphere as in figure 1.1. Note that the Bloch space does not represent the complex Hilbert space itself.

More generally, we can choose any pair of orthonormal states to form our computational basis. On the bloch sphere, this corresponds to any two vectors pointing in opposite directions. One such computational basis if formed by the $|+\rangle = \frac{1}{\sqrt{2}}(|0\rangle + |1\rangle)$ and $|-\rangle = \frac{1}{\sqrt{2}}(|0\rangle - |1\rangle)$ states.
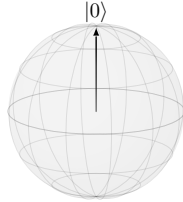
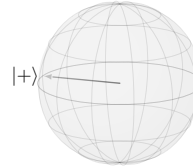**Figure 1.1:** $|0\rangle$ basis state **Figure 1.2:** $|+\rangle$ basis state

Any qubit $|\psi\rangle$ can be represented as complex linear combination of the chosen basis, provided that the qubit state vector is normalised.

$$|\psi\rangle = \alpha\,|0\rangle + \beta\,|1\rangle \qquad |\alpha|^2 + |\beta|^2 = 1 \qquad \alpha, \beta \in \mathbb{C}$$

Multiple Qubit States

Suppose we have n qubits. By taking the Kronecker product, we can construct 2^n computational basis states.

$$|00\dots00\rangle = |0\rangle_n \otimes |0\rangle_{n-1} \otimes \cdots \otimes |0\rangle_1 \otimes |0\rangle_0$$

$$\dots$$

$$|11\dots11\rangle = |1\rangle_n \otimes |1\rangle_{n-1} \otimes \cdots \otimes |1\rangle_1 \otimes |1\rangle_0$$

Figure 1.3: 2^n computational basis states.

It follows then that any complex linear combination of the computational basis states is also a valid qubit state.

$$|\psi\rangle = \alpha_{00\dots00} |00\dots00\rangle + \alpha_{00\dots01} |00\dots01\rangle + \cdots + \alpha_{11\dots11} |11\dots11\rangle$$

Whilst the Bloch sphere representation of a single qubit is incredibly useful, there is no easy generalisation of the Bloch sphere for multiple qubit states [5].

Quantum Gates

1.2 Electronic Structure Theory

Electronic Structure Problem

References: [6]

The main interest of electronic structure theory is finding approximate solutions to the eigenvalue equation of the full molecular Hamiltonian. Specifically, we seek solutions to the non-relativistic time-independent Schrödinger equation.

$$H = -\sum_{i=1}^{N} \frac{1}{2}\nabla_i^2 - \sum_{i=1}^{M} \frac{1}{2M_i}\nabla_i^2 - \sum_{i=1}^{N}\sum_{j=1}^{M} \frac{Z_j}{|r_i - R_j|} + \sum_{i=1}^{N}\sum_{j>i}^{N} \frac{1}{|r_i - r_j|} + \sum_{i=1}^{M}\sum_{j>i}^{M} \frac{Z_i Z_j}{|R_i - R_j|}$$

Figure 1.4: Full molecular Hamiltonian in atomic units, where Z_i is the charge of nucleus i and M_i is its mass relative to the mass of an electron.

The full molecular Hamiltonian, H, describes all interactions within a system of N interacting electrons and M nuclei. The first term corresponds to the kinetic energy of all electrons in the system. The second term corresponds to the total kinetic energy of all nuclei. The third term corresponds to the pairwise attractive Coulombic interactions between the N electrons and M nuclei, whilst the fourth and fifth terms correspond to all repulsive Coulombic interactions between electrons and nuclei respectively.

We are able to simplify the problem to an electronic one using the Born-Oppenheimer approximation. Motivated by the large difference in mass of electrons and nuclei, we can approximate the nuclei as stationary on the timescale of electronic motion such that the electronic wavefunction depends only parametrically on the nuclear coordinates. The full molecular wavefunction can then be expressed as an adiabatic separation as below.

$$\Phi_{\text{total}} = \psi_{\text{elec}}(\{r\}; \{R\})\, \psi_{\text{nuc}}(\{R\})$$

Within this approximation, the nuclear kinetic energy term can be neglected and the nuclear repulsive term is considered to be constant. Since constants in

eigenvalue equations have no effect on the eigenfunctions and simply add to the resulting eigenvalue, we will omit this too. The resulting equation is the electronic Hamiltonian for N electrons.

$$H = -\sum_{i=1}^{N} \frac{1}{2}\nabla_i^2 - \sum_{i=1}^{N}\sum_{j=1}^{M} \frac{Z_j}{|r_i - R_j|} + \sum_{i=1}^{N}\sum_{j>i}^{N} \frac{1}{|r_i - r_j|}$$

Figure 1.5: Electronic molecular Hamiltonian in atomic units.

Throughout the remainder of this text, we will concern ourselves only with the electronic Hamiltonian, simply referring to it as the Hamiltonian, H. The solution to the eigenvalue equation involving the electronic Hamiltonian is the electronic wavefunction, which depends only parametrically on the nuclear coordinates. It is solved for fixed nuclear coordinates, such that different arrangements of nuclei yields different functions of the electronic coordinates. The total molecular energy can then be calculated by solving the electronic Schrödinger equation and including the constant repulsive nuclear term.

$$E_{\text{total}} = E_{\text{elec}} + \sum_{i=1}^{M}\sum_{j>i}^{M} \frac{Z_i Z_j}{|R_i - R_j|}$$

Many-Electron Wavefunctions

References: [6]

The many-electron wavefunction, which describes all fermions in given molecular system, must satisfy the Pauli principle. This is an independent postulate of quantum mechanics that requires the many-electron wavefunction to be antisymmetric with respect to the exchange of any two fermions.

A spatial molecular orbital is defined as a one-particle function of the position vector, spanning the whole molecule. The spatial orbitals form an orthonormal set $\{\psi_i(\mathbf{r})\}$, which if complete can be used to expand any arbitrary single-particle molecular wavefunction, that is, an arbitrary single-particle function of the position vector. In practice, only a finite set of such orbitals is available to us, spanning only

a subspace of the complete space. Hence, wavefunctions expanded using this finite set are described as being 'exact' only within the subspace that they span.

We will now introduce the spin orbitals $\{\phi_i(\mathbf{x})\}$, that is, the set of functions of the composite coordinate $\mathbf{x}$, which describes both the spin and spatial distribution of an electron. Given a set of K spatial orbitals, we can construct $2K$ spin orbitals by taking their product with the orthonormal spin functions $\alpha(\omega)$ and $\beta(\omega)$. Whilst the Hamiltonian operator makes no reference to spin, it is a necessary component when constructing many-electron wavefunctions in order to correctly antisymmetrise the wavefunction with respect to fermion exchange. Constructing the antisymmetric many-electron wavefunction from a finite set of spin orbitals amounts to taking the appropriate linear combinations of symmetric products of N spin orbitals known as Hatree products.

$$\psi_{1,2}(\mathbf{x_1}, \mathbf{x_2}) = \phi_i(\mathbf{x_1})\phi_j(\mathbf{x_2}) \qquad \psi_{2,1}(\mathbf{x_2}, \mathbf{x_1}) = \phi_i(\mathbf{x_2})\phi_j(\mathbf{x_1})$$

$$\Psi_{1,2}(\mathbf{x_1}, \mathbf{x_2}) = \frac{1}{\sqrt{2}}\left[\psi_{1,2}(\mathbf{x_1}, \mathbf{x_2}) - \psi_{2,1}(\mathbf{x_2}, \mathbf{x_1})\right]$$

Figure 1.6: Symmetric Hartree products $\psi_{1,2}(\mathbf{x_1}$ and $\mathbf{x_2})$, $\psi_{2,1}(\mathbf{x_2}, \mathbf{x_1})$, and their antisymmetric linear combination $\Psi_{1,2}(\mathbf{x_1}, \mathbf{x_2})$.

A general procedure for this is achieved by constructing a Slater determinant from the finite set of spin orbitals, where each row relates to the electron coordinate $\mathbf{x_n}$ and each column corresponds to a particular spin orbital ϕ_i.

$$\psi(\mathbf{x}_1, \mathbf{x}_2) = \frac{1}{\sqrt{N!}} \begin{vmatrix} \phi_i(\mathbf{x}_1) & \phi_j(\mathbf{x}_1) & \ldots & \phi_k(\mathbf{x}_1) \\ \phi_i(\mathbf{x}_2) & \phi_j(\mathbf{x}_2) & \ldots & \phi_k(\mathbf{x}_2) \\ \vdots & \vdots & & \vdots \\ \phi_i(\mathbf{x}_N) & \phi_j(\mathbf{x}_N) & \ldots & \phi_k(\mathbf{x}_N) \end{vmatrix}$$

Figure 1.7: Slater determinant representing an antisymmetrised N-electron wavefunction.

Since exchanging any two rows or columns of a determinant changes its sign, Slater determinants satisfy the Pauli principle by definition. Slater determinants

constructed from orthonormal spin orbitals are themselves normalised and N electron Slater determinants constructed from different orthonormal spin orbitals are orthogonal to one another [6].

By constructing Slater determinants and antisymmetrising the many-electron wavefunction to meet the requirements of the Pauli principle, we have incorporated exchange correlation, in that, the motion of two electrons with parallel spins is now correlated.

The Hartree-Fock method yields a set of orthonormal spin orbitals, which when used to construct a single Slater determinant, gives the best variational approximation to the ground state of a system [6]. By treating electron-electron repulsion in an average way, the Hartree-Fock approximation allows us to iteratively solve the Hartree-Fock equation for spin orbitals until they become the same as the eigenfunctions of the Fock operator. This is known as the Self-Consistent Field (SCF) method and is an elegant starting point for finding approximate solutions to the many-electron wavefunction.

$$\left[-\frac{1}{2}\nabla^2 - \sum_{A=1}^{M} \frac{Z_A}{r_{i_A}} + \mathbf{v}^{\text{HF}}(i) \right] \phi_i(\mathbf{x}_i) = \varepsilon \phi_i(\mathbf{x}_i)$$

Figure 1.8: Hartree-Fock equation.

For an N electron system, and given a set of $2K$ Hartree-Fock spin orbitals, where $2K > N$, there exist many different single Slater determinants. The Hartree-Fock groundstate being one of these. The remainder are excited Slater determinants, recalling that all of these must be orthogonal to one-another. By treating the Hartree-Fock ground state as a reference state, we can describe the excited states relative to the reference state, as single, double, ..., N-tuple excited states [6].

Second Quantisation

References: [7], [8]

1. Background

In second quantisation, both observables and states (by acting on the vacuum state) are represented by operators, namely the creation and annhilation operators [7]. In contrast to the standard formulation of quantum mechanics, operators in second quantisation incorporate the relevant Bose or Fermi statistics each time they act on a state, circumventing the need to keep track of symmetrised or antisymmetrised products of single-particle wavefunctions [8]. Put differently, the antisymmetry of an electronic wavefunction simply follows from the algebra of the creation and annhilation operators [7], which greatly simplifies the discussion of systems of many identical interacting fermions [8].

The Fock space is a linear abstract vector space spanned by N orthonormal occupation number vectors [7], each representing a single Slater determinant. Hence, given a basis of N spin orbitals we can construct 2^N single Slater determinants, each corresponding to a single occupation number vector in the full Fock space.

The occupation number vector for fermionic systems is succinctly denoted in Dirac notation as below, where the occupation number f_j is 1 if spin orbital j is occupied, and 0 if spin orbital j is unnoccupied.

$$|\psi\rangle = |f_{n-1} \ f_{n-2} \ldots f_1 \ f_0\rangle \qquad \text{where } f_j \in 0, 1$$

Whilst there is a one-to-one mapping between Slater determinants with canonically ordered spin orbitals and the occupation number vectors in the Fock space, it is important to distinguish between the two since, unlike the Slater determinants, the occupation number vectors have no spatial structure and are simply vectors in an abstract vector space. [7].

Creation and Annhilation Operators

References: [7]

Operators in second quantisation are constructed from the creation and annhilation operators $a_j^\dagger$ and a_j, where the subscripts i and j denote the spin orbital. $a_j^\dagger$ and a_j are one another's Hermitian adjoints, and are not self-adjoint [7].

Taking the excitation of an electron from spin orbital 0 to spin orbital 1 as an example, we can construct the following excitation operator.

$$a_1^\dagger a_0 \left|0\ldots01\right\rangle = \left|0\ldots10\right\rangle$$

Due to the fermionic exchange anti-symmetry imposed by the Pauli principle, the action of the creation and annhilation operators introduces a phase to the state that depends on the parity of the spin orbitals preceding the target spin orbital.

$$a_j^\dagger \left|f_{n-1}\ldots f_{j+1},\ 0,\ f_{j-1}\ldots f_0\right\rangle = (-1)^{\sum_{s=0}^{j-1} f_s} \left|f_{n-1}\ldots f_{j+1},\ 1,\ f_{j-1}\ldots f_0\right\rangle$$

$$a_j \left|f_{n-1}\ldots f_{j+1},\ 1,\ f_{j-1}\ldots f_0\right\rangle = (-1)^{\sum_{s=0}^{j-1} f_s} \left|f_{n-1}\ldots f_{j+1},\ 0,\ f_{j-1}\ldots f_0\right\rangle$$

In second quantisation, this exchange anti-symmetry requirement is accounted for by the anti-commutation relations of the creation and annhilation operators.

$$\{\hat{a}_j, \hat{a}_k\} = 0 \qquad \{\hat{a}_j^\dagger, \hat{a}_k^\dagger\} = 0 \qquad \{\hat{a}_j, \hat{a}_k^\dagger\} = \delta_{jk}\hat{1}$$

Figure 1.9: Anti-commutation relations of fermionic creation and annhilation operators.

The phase factor required for the second quantised representation to be consistent with the first quantised representation is automatically kept track of by the anticommutation relations of the creation and annhilation operators [7].

Hamiltonian in Second Quantisation

The Hamiltonian in second quantisation is constructed from creation and annhilation operators as follows.

$$\hat{H} = \sum_{ij} h_{ij} a_i^\dagger a_j + \frac{1}{2}\sum_{ijkl} h_{ijkl} a_i^\dagger a_j^\dagger a_k a_l + h_{\mathrm{Nu}}$$

Where the one-body matrix element h_{ij} corresponds to the kinetic energy of an electron and its interaction energy with the nuclei, and the two-body matrix element h_{ijkl} corresponds to the repulsive interaction between electrons i and j.

$$h_{ij} = \int_{-\infty}^{\infty} \psi_{i(x_1)}^* \left(-\frac{1}{2}\nabla^2 + \hat{V}_{(x_1)}\right) \psi_{j(x_1)}\ d^3 x_1$$

1. Background

$$h_{ijkl} = \int_{-\infty}^{\infty} \int_{-\infty}^{\infty} \psi_{i(x_1)}^* \psi_{j(x_2)}^* \left(\frac{1}{|x_1 - x_2|} \right) \psi_{k(x_2)} \psi_{l(x_1)} \ d^3 x_1 d^3 x_2$$

h_{Nu} is a constant corresponding to the repulsive interaction between nuclei. These matrix elements are computed classically, allowing us to simulate only the inherently quantum aspects of the problem on a quantum computer.

1.3   Variational Quantum Eigensolver

References: [9], [3], [10]

Fermion-Qubit Encodings

References: [11]

In order to represent the fermionic wavefunction on a quantum computer, we must first create a mapping between the fermionic state vector and the qubit state vector. There are a number of fermion-qubit encodings used today including the Jordan-Wigner transformation, Bravyi-Kitaev transformation and the Parity mapping. Whilst the Bravyi-Kitaev transformation and Parity mappings can more efficiently encode the fermionic wavefunction in some ways, we will only consider the Jordan-Wigner transformation for the remainder of this text as its simplicity provides us with a more intuitive picture of the computation.

The form of the occupation number representation vector and the qubit statevector suggests the following identification between electronic states and qubit states.

$$|f_{n-1} \ldots f_0\rangle \quad \rightarrow \quad |q_{n-1} \ldots q_0\rangle$$

That is, we allow each qubit to store the occupation number of a given spin-orbital. Hence, in order to actually simulate a Hamiltonian we must map the fermionic creation and annhilation operators onto qubit operators, and these operators must behave in the same way as their fermionic analogues.

$$\hat{Q}^+ |0\rangle = |1\rangle \qquad \hat{Q}^+ |1\rangle = 0 \qquad \hat{Q} |1\rangle = |0\rangle \qquad \hat{Q} |0\rangle = 0$$

The qubit operators must also preserve the fermionic anti-commutation relations in order to satisfy the Pauli antisymmetry requirement.

$$\{\hat{Q}_j, \hat{Q}_k\} = 0 \qquad \{\hat{Q}_j^\dagger, \hat{Q}_k^\dagger\} = 0 \qquad \{\hat{Q}_j, \hat{Q}_k^\dagger\} = \delta_{jk}$$

One such qubit encoding is known as the Jordan-Wigner transformation. It expresses the fermionic creation and annhilation operators as a linear combination of the

Pauli matrices.

$$\hat{Q}^+ = |1\rangle \langle 0| = \frac{1}{2}(X - iY) \qquad \hat{Q} = |0\rangle \langle 1| = \frac{1}{2}(X + iY)$$

When dealing with **multiple-qubits**, we must also account for the occupation parity of the qubits preceding the target qubit j.

$$a_j^\dagger |f_{n-1} \dots f_{j+1}, \ 0, \ f_{j-1} \dots f_0\rangle = (-1)^{\sum_{s=0}^{j-1} f_s} |f_{n-1} \dots f_{j+1}, \ 1, \ f_{j-1} \dots f_0\rangle$$

We do this by introducing a string of Pauli Z operators that computes the parity of the qubits preceding the target qubit.

$$\hat{a}_j^+ = \frac{1}{2}(X - iY) \prod_{k=1}^{j-1} Z_k \qquad \hat{a}_j = \frac{1}{2}(X + iY) \prod_{k=1}^{j-1} Z_k$$

Where $\prod$ is the tensor product.

A more compact notation is,

$$\hat{a}_j^+ = \frac{1}{2}(X - iY) \otimes Z_{j-1}^{\rightarrow} \qquad \hat{a}_j = \frac{1}{2}(X + iY) \otimes Z_{j-1}^{\rightarrow}$$

Where $Z_i^{\rightarrow}$ is the parity operator with eigenvalues ± 1, and ensures the correct phase is added to the qubit state vector.

$$Z_i^{\rightarrow} = Z_i \otimes Z_{i-1} \otimes \cdots \otimes Z_0$$

For instance, the creation operator $a_3^\dagger$ maps to the following Pauli string,

$$\hat{a}_3^\dagger = \frac{1}{2}(X_3 - iY_3) \otimes Z_2 \otimes Z_1 \otimes Z_0$$
$$\hat{a}_3^\dagger = \frac{1}{2}(X_3 \otimes Z_2 \otimes Z_1 \otimes Z_0) - \frac{1}{2}i(Y_3 \otimes Z_2 \otimes Z_1 \otimes Z_0)$$

Usually we drop the subscript specifying the orbital acted on.

Unitary Coupled Cluster

Whilst unitary coupled cluster theory was proposed in X, interest in its applications has been minimal due to the inability of classical computers to efficiently evaluate its equations. As suggested by Peruzzo et al [12], the UCC formulation of a

wavefunction can be efficiently implemented on a quantum computer using quantum gates.

Unitary coupled cluster theory allows us to represent an arbitrary state $|\psi\rangle$ using the following exponential ansatz.

$$|\psi\rangle = e^{\hat{T}(\theta)-\hat{T}^{\dagger}(\theta)} |\psi_0\rangle$$

Where $|\psi_0\rangle$ is a single reference Slater determinant, usually the Hartree-Fock groundstate obtained via the self-consistent field method. The exponential operator $U(\theta) = e^{\hat{T}(\theta)-\hat{T}^{\dagger}(\theta)}$ is unitary since its exponent $\hat{T}(\theta) - \hat{T}^{\dagger}(\theta)$ is anti-Hermitian.

The excitation operators are given by

$$\hat{T}(\theta) - \hat{T}^{\dagger}(\theta) = \sum_{i,a} \theta_i^a (a_i^{\dagger} a_a - a_a^{\dagger} a_i) + \sum_{i,j,a,b} \theta_{ij}^{ab}(a_i^{\dagger} a_j^{\dagger} a_a a_b - a_a^{\dagger} a_b^{\dagger} a_i a_j) + \dots$$

Where i, j indexes occupied spin orbitals and a, b indexes virtual, or unoccupied, spin orbitals. The resulting unitary operator $U(\theta)$ cannot be directly implemented on a quantum computer since the terms of the excitation operator do not commute. Instead, we must invoke the Trotter formula to approximate the unitary.

$$e^{A+B} = (e^A e^B)^{\rho}$$

Taking a single Trotter step $\rho = 1$, we obtained the disentangled UCC

$$U_{t1}(\theta) = \prod_m e^{\theta_m(\tau_m - \tau_m^{\dagger})} \tag{1.1}$$

Where m indexes all possible excitations. It has been shown in [13] that the disentangled UCC can exactly parametrise any state.

"In practice, the excitations are truncated to only include single and double excitations. This UCCSD ansatz has been popular in the VQE literature and is often the benchmark for more cost effective methods." [10].

1. Background

"Only UCCSD excitation operators which conserve spin were used for ansatz construction. Ansatze generated in this manner preserve the spin symmetry of the spin reference" [10]

—

In this chapter we introduce we introduce Unitary Coupled Cluster theory which will serve as the basis for the Variational Quantum Eigensolver algorithm introduced in chapter XXX. In particular, we are interested in developing the Unitary-Product State which will serve as a variational ansatz.

One notable advantage of the VQE algorithm is its ability to be run on any quantum architecture, moreover, we can leverage architecture requirements when designing the variational ansatz. [3].

"Even in the event that some error correction is required to exceed current computational capabilities, this same robustness may translate to requiring minimal error cor- rection resources when compared with other algorithms." [3]

We begin by...

Within the traditional coupled-cluster framework, the ground electronic state is prepared by applying the CC operator to a reference state (usually Hartree-Fock).

$$|\psi\rangle = e^{\hat{T}} |\phi_0\rangle$$

Where $\hat{T}$ is the cluster excitation operator.

Quantum gates, however, must be unitary operators, so instead, we work within the UCC framework.

$$|\psi\rangle = e^{\hat{T}} |\phi_0\rangle$$

Where $\hat{T}$ is now an **anti-Hermitian** operator, and $e^{\hat{T}}$ is unitary.

In general, we can prepare exact electronic states by applying a sequence of k parametrised unitary operators to our reference state.

$$|\psi\rangle = \prod_i^k U_i(\theta_i) |\phi_0\rangle$$

Where $U_i(\theta_i)$ is a parametrised unitary operator

The parameters θ_i are then optimised to find the ground state energy.

General fermionic single and double excitation operators are defined as,

$$a_q^\dagger a_p \text{ and } a_r^\dagger a_s^\dagger a_q a_p$$

Exciting one electron from p to q, and two electrons from p, q to r, s respectively.

Taking a linear combination of these, we obtain **anti-Hermitian** fermionic single and double excitation operators.

$$\hat{\kappa}_p^q = a_q^\dagger a_p - a_p^\dagger a_q$$

$$\hat{\kappa}_{pq}^{rs} = a_r^\dagger a_s^\dagger a_q a_p - a_p^\dagger a_q^\dagger a_s a_r$$

Such that upon exponentiating, we obtain **unitary** operators.

$$U_p^q = e^{\hat{\kappa}_p^q} \qquad U_{pq}^{rs} = e^{\hat{\kappa}_{pq}^{rs}}$$

Variational Quantum Eigensolver

Recalling the Jordan-Wigner encoding for the creation and annhilation operators,

$$\hat{a}_j^+ = \frac{1}{2}(X - iY) \otimes Z_{j-1}^{\rightarrow} \qquad \hat{a}_j = \frac{1}{2}(X + iY) \otimes Z_{j-1}^{\rightarrow}$$

1. Background

The anti-Hermitian fermionic single and double excitation operators κ_p^q and κ_{pq}^{rs}

$$F_p^q = \frac{i}{2}(Y_p X_q - X_p Y_q) \prod_{k=p+1}^{q-1} Z_k$$

$$F_{pq}^{rs} = \frac{i}{8}(X_p X_q Y_s X_r + Y_p X_q Y_s Y_r + X_p Y_q Y_s Y_r + X_p X_q X_s Y_r -$$

$$Y_p X_q X_s X_r - X_p Y_q X_s X_r - Y_p Y_q Y_s X_r - Y_p Y_q X_s Y_r) \prod_{k=p+1}^{q-1} Z_k \prod_{l=r+1}^{s-1} Z_l$$

Multiplying by θ and exponentiating yields the parametrised unitary qubit operators,

$$U_p^q(\theta) = \exp\left(i\frac{\theta}{2}(Y_p X_q - X_p Y_q) \prod_{k=p+1}^{q-1} Z_k \right)$$

$$U_{pq}^{rs}(\theta) = \exp\left(i\frac{\theta}{8}(X_p X_q Y_s X_r + \cdots - Y_p Y_q Y_s X_r - Y_p Y_q X_s Y_r) \prod_{k=p+1}^{q-1} Z_k \prod_{l=r+1}^{s-1} Z_l \right)$$

To summarise, we constructed anti-Hermitian single and double excitation operators from a linear combination of fermionic excitation operators,

$$\hat{\kappa}_p^q = a_q^\dagger a_p - a_p^\dagger a_q \qquad \hat{\kappa}_{pq}^{rs} = a_r^\dagger a_s^\dagger a_q a_p - a_p^\dagger a_q^\dagger a_s a_r$$

We then mapped these to qubit operators using the Jordan-Wigner transformation,

$$\hat{\kappa}_p^q \xrightarrow{\text{JW}} F_p^q \qquad\qquad \hat{\kappa}_{pq}^{rs} \xrightarrow{\text{JW}} F_{pq}^{rs}$$

And finally, we exponentiated to yield the parametrised unitary qubit operators.

$$U_p^q(\theta) = e^{\theta_p^q F_p^q} \qquad U_{pq}^{rs}(\theta) = e^{\theta_{pq}^{rs} F_{pq}^{rs}}$$

Let's look again at the parametrised single-body unitary operator,

$$U_p^q(\theta) = \exp\left(i\frac{\theta}{2}(Y_p X_q - X_p Y_q) \prod_{k=p+1}^{q-1} Z_k \right)$$

$$U_p^q(\theta) = \left(\exp\left[i\frac{\theta}{2} Y_p X_q \prod_{k=p+1}^{q-1} Z_k \right] \right)\left(\exp\left[-i\frac{\theta}{2} X_p Y_q \prod_{k=p+1}^{q-1} Z_k \right] \right)$$

The first exponential term can be implemented by the following phase gadget.

$$\exp\left(i\frac{\theta}{2}Y_pX_q\prod_{k=p+1}^{q-1}Z_k\right)$$

Left CNOT ladder construction calculates the parity of the qubit state, and applies a rotation in the Z basis if the parity is odd.

Whilst the second exponential term can be implemented by the phase gadget.

$$\exp\left(-i\frac{\theta}{2}X_pY_q\prod_{k=p+1}^{q-1}Z_k\right)$$

Together, they constitute the single-body unitary excitation operator $U_p^q(\theta)$

By defining the ordering of spin-orbitals such that adjacent spin-orbitals share the same spatial orbital, adjacent single-body operators commute.

$$\left[\hat{\kappa}_p^q, \hat{\kappa}_{p+1}^{q+1}\right] = 0$$

The same is therefore true for the resulting qubit operators,

$$\left[F_p^q, F_{p+1}^{q+1}\right] = 0$$

$$p, q \in \text{even} \qquad p+1, q+1 \in \text{odd}$$

This allows us to define the parametrised unitary qubit operators in terms of spin-adapted excitation operators.

$$U_p^q(\theta) = \exp\left[\theta\left(F_p^q + F_{p+1}^{q+1}\right)\right]$$

In other words, since F_p^q and F_{p+1}^{q+1} commute, we can think of them as a single operator with a single parameter.

Chapter 2

ZX Calculus

The ZX calculus is a diagrammatic language for reasoning about quantum processes LALALA

We will then introduce the rewrite rules... that come equipped with the ZX calculus. These rules extend the ZX calculus from notation into a language.

Notation - flow of time goes from left to right - global scalar factor

Note that in this text, we will interpret the flow of time from left to right. Whilst we obtain the correct states, we obtain the wrong scalar factor. For the remainder of this thesis, we will ignore global non-zero scalar factors. Hence, equal signs should be interpreted as 'equal up to a global phase'.

All the diagrams in this chapter also hold for the colour-swapped counterparts.

2.1 Generators

By sequentially or horizontally composing the *Z Spider* (green) and *X Spider* (red) generators, we can construct undirected multigraphs known as ZX diagrams [14]. That is, graphs that allow multiple edges between vertices. Since *only connectivity matters* in the ZX calculus, a valid ZX diagram can be arbitrarily deformed, provided that the order of inputs and outputs is preserved.
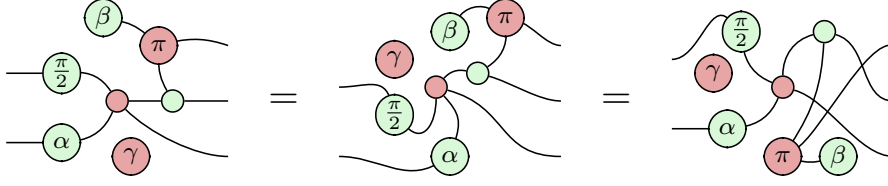
Figure 2.1: Three equivalent ZX diagrams (*only connectivity matters*).

Z Spiders (green) are defined with respect to the *Z* eigenbasis ($|0\rangle$ and $|1\rangle$) such that a Z Spider with n inputs and m outputs represents the following linear map.

$$ n \vdots \underset{\alpha}{\bigcirc} \vdots m \; = \; |0\rangle^{\otimes m} \langle 0|^{\otimes n} + e^{i\alpha} |1\rangle^{\otimes m} \langle 1|^{\otimes n} $$

Figure 2.2: Interpretation of a Z Spider as a linear map.

X Spiders (red), are defined with respect to the *X* eigenbasis ($|+\rangle$ and $|-\rangle$).

$$ n \vdots \underset{\alpha}{\bigcirc} \vdots m \; = \; |+\rangle^{\otimes m} \langle +|^{\otimes n} + e^{i\alpha} |-\rangle^{\otimes m} \langle -|^{\otimes n} $$

Figure 2.3: Interpretation of an X Spider as a linear map.

We can represent the *Z* eigenstates, $|0\rangle$ and $|1\rangle$, using an *X* spider with a phase of either 0 or π.

$$ \bigcirc\!\!- \; = \; |+\rangle + |-\rangle = \sqrt{2}\,|0\rangle \qquad\qquad \underset{\pi}{\bigcirc}\!\!- \; = \; |+\rangle - |-\rangle = \sqrt{2}\,|1\rangle $$

Figure 2.4: $|0\rangle$ eigenstate **Figure 2.5:** $|1\rangle$ eigenstate

Similarly, we can represent the X eigenstates, $|+\rangle$ and $|-\rangle$, using the corresponding Z spiders.

$$\text{⬭}— = |0\rangle + |1\rangle = \sqrt{2}\,|+\rangle \qquad \text{⬭}_\pi— = |0\rangle - |1\rangle = \sqrt{2}\,|-\rangle$$

Figure 2.6: $|+\rangle$ eigenstate   **Figure 2.7:** $|-\rangle$ eigenstate

Single qubit rotations in the Z basis are represented by a Z Spider with a single input and a single output. Arbitrary rotations in the X basis are represented by the corresponding X spider. We can view these as rotations of the Bloch sphere.

$$—\,\alpha\,— \quad |0\rangle\langle 0| + e^{i\alpha}|1\rangle\langle 1| = \begin{pmatrix} 1 & 0 \\ 0 & e^{i\alpha} \end{pmatrix} \rightarrow$$

$$—\,\alpha\,— \quad |+\rangle\langle +| + e^{i\alpha}|-\rangle\langle -| = \frac{1}{2}\begin{pmatrix} 1 + e^{i\alpha} & 1 - e^{i\alpha} \\ 1 - e^{i\alpha} & 1 + e^{i\alpha} \end{pmatrix} \rightarrow$$

We can recover the Pauli Z and Pauli X matrices by setting the angle $\alpha = \pi$.

$$—\,\pi\,— \; = |0\rangle\langle 0| + e^{i\pi}|1\rangle\langle 1| = \begin{pmatrix} 1 & 0 \\ 0 & -1 \end{pmatrix}$$

$$—\,\pi\,— \; = |+\rangle\langle +| + e^{i\pi}|-\rangle\langle -| = \begin{pmatrix} 0 & 1 \\ 1 & 0 \end{pmatrix}$$

Figure 2.8: Pauli Z and X gates in the ZX calculus.

Composition

To calculate the matrix of a ZX diagram consisting of sequentially composed spiders, we take the matrix product. Note that the order of operation of matrix multiplication is the reverse as in the ZX diagram as we have defined it.

$$—\,\alpha\,—\,\beta\,—\,\gamma\,— \; = \begin{pmatrix} 1 & 0 \\ 0 & e^{i\gamma} \end{pmatrix}\begin{pmatrix} 1 + e^{i\beta} & 1 - e^{i\beta} \\ 1 - e^{i\beta} & 1 + e^{i\beta} \end{pmatrix}\begin{pmatrix} 1 & 0 \\ 0 & e^{i\alpha} \end{pmatrix}$$

2. ZX Calculus

Alternatively, we could have chosen to compose the spiders in parallel, resulting in the tensor product.

$$\begin{array}{c}\alpha \\ \beta\end{array} = \begin{pmatrix} 1 & 0 \\ 0 & e^{i\alpha} \end{pmatrix} \otimes \begin{pmatrix} 1 + e^{i\beta} & 1 - e^{i\beta} \\ 1 - e^{i\beta} & 1 + e^{i\beta} \end{pmatrix}$$

The CNOT gate in the ZX calculus is represented by a Z spider (control qubit) and an X spider (target qubit). We can arbitrarily deform the diagram and decompose it into matrix and tensor products as follows.

$$\begin{array}{c} \text{(diagram)} \end{array} = \begin{array}{c} \text{(diagram)} \end{array} = \boxed{A} \quad \boxed{B}$$
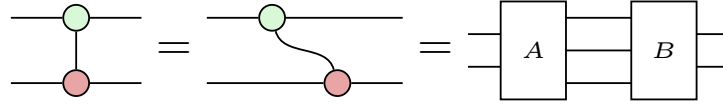
We can calculate matrix A, consisting of a single-input and two-output Z Spider (4×2 matrix) and an empty wire (identity matrix), by taking the tensor product.

$$\boxed{A} = \begin{array}{c} \text{(diagram)} \end{array} = \begin{pmatrix} 1 & 0 \\ 0 & 0 \\ 0 & 0 \\ 0 & 1 \end{pmatrix} \otimes \begin{pmatrix} 1 & 0 \\ 0 & 1 \end{pmatrix}$$

Similarly, to calculate the matrix B, we take the following tensor product.

$$\boxed{B} = \begin{array}{c} \text{(diagram)} \end{array} = \begin{pmatrix} 1 & 0 \\ 0 & 1 \end{pmatrix} \otimes \frac{1}{\sqrt{2}} \begin{pmatrix} 1 & 0 & 0 & 1 \\ 0 & 1 & 1 & 0 \end{pmatrix}$$

We can then calculate the CNOT matrix by taking the matrix product of matrix A and matrix B as follows.

$$\begin{array}{c} \text{(diagram)} \end{array} = \left[\begin{pmatrix} 1 & 0 \\ 0 & 1 \end{pmatrix} \otimes \frac{1}{\sqrt{2}} \begin{pmatrix} 1 & 0 & 0 & 1 \\ 0 & 1 & 1 & 0 \end{pmatrix} \right] \left[\begin{pmatrix} 1 & 0 \\ 0 & 0 \\ 0 & 0 \\ 0 & 1 \end{pmatrix} \otimes \begin{pmatrix} 1 & 0 \\ 0 & 1 \end{pmatrix} \right] \simeq \begin{pmatrix} 1 & 0 & 0 & 0 \\ 0 & 1 & 0 & 0 \\ 0 & 0 & 0 & 1 \\ 0 & 0 & 1 & 0 \end{pmatrix}$$

Since *only connectivity matters* (2.1), we could have equivalently calculated the matrix of the CNOT gate by deforming the diagram as follows.
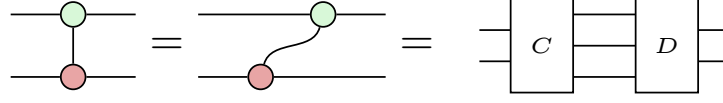
Had we chosen to make the first qubit the target and the second qubit the control, we would have obtained the following.

$$\text{(diagram)} = \left[\frac{1}{\sqrt{2}} \begin{pmatrix} 1 & 0 & 0 & 1 \\ 0 & 1 & 1 & 0 \end{pmatrix} \otimes \begin{pmatrix} 1 & 0 \\ 0 & 1 \end{pmatrix} \right] \left[\begin{pmatrix} 1 & 0 \\ 0 & 1 \end{pmatrix} \otimes \begin{pmatrix} 1 & 0 \\ 0 & 0 \\ 0 & 0 \\ 0 & 1 \end{pmatrix} \right] \simeq \begin{pmatrix} 1 & 0 & 0 & 0 \\ 0 & 0 & 0 & 1 \\ 0 & 0 & 1 & 0 \\ 0 & 1 & 0 & 0 \end{pmatrix}$$

Hadamard Generator

All quantum gates are unitary transformations. Therefore, up to a global phase, an arbitrary single qubit rotation U can be viewed as a rotation of the Bloch sphere about some axis. We can decompose the unitary U using Euler angles to represent the rotation as three successive rotations [14].
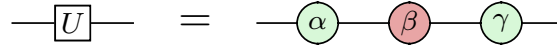
Figure 2.9: Arbitrary single-qubit rotation.

Recall that the Hadamard gate H switches between the $|0\rangle/|1\rangle$ and $|+\rangle/|-\rangle$ bases. That is, it corresponds to a rotation of the Bloch sphere π radians about the line bisecting the Z and X axes.

There are many equivalent ways of decomposing the Hadamard gate H using Euler angles. By choosing $\alpha = \beta = \gamma = \frac{\pi}{2}$, we obtain H up to a global phase of $\exp(-i\pi/4)$. See Appendix 7.2 for other definitions.

Figure 2.10: Definition of the Hadamard generator.

2.2 Rewrite Rules

Spider Fusion

The most fundamental rule of the ZX calculus is the *spider fusion* rule [14]. It states that two spiders connected by one or more wires fuse if they are the same colour. It is the generalisation of adding the phases of successive rotations of the Bloch sphere. Since we interpret the phases α and β as $e^{i\alpha}$ and $e^{i\beta}$, it follows that the phase $\alpha + \beta$ is modulo 2π.
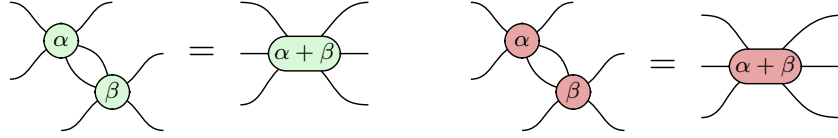
Figure 2.11: Spider fusion rule for Z spiders (left) and X spiders (right).

We can use this rule to identify commutation relations such as Z rotations commuting through CNOT controls, and X rotations, through CNOT targets.
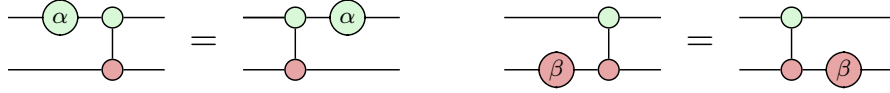
Identity Removal

The *identity removal* rule states that any two-legged spider with no phase $(\alpha = 0)$ is equivalent to a rotation by 0 radians, or identity.
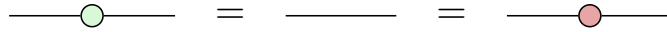
Figure 2.12: Identity removal rule.

Combining this with the spider fusion rule (2.11), we see that two successive rotations with opposite phases is equivalent to an empty wire.
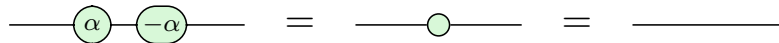
State Copy and π Copy Rules

We can depict the Z and X eigenstates by assigning a phase to a Z or an X spider, respectively, through a Boolean variable a (0 or 1) multiplied by π [14].

$$\text{(a\pi)}— \; = |0\rangle \; \text{ where } a = 0 \text{ and } |1\rangle \; \text{ where } a = 1$$

$$\text{(a\pi)}— \; = |+\rangle \; \text{ where } a = 0 \text{ and } |-\rangle \; \text{ where } a = 1$$

The π *copy* rule states that when a Pauli Z or Pauli X gate is pushed through a spider of the opposite colour, it is copied on all other legs and negates the spider's phase. A similar *state copy* rule applies to the Z and X eigenstates.
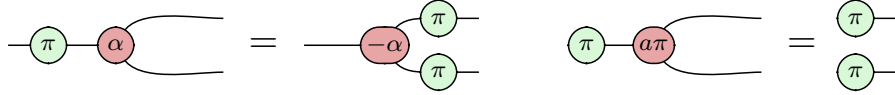
Figure 2.13: π copy (left) and state copy (right) rules for Pauli Z gate and Z eigenstates.

Bialgebra Rule

Using the spider fusion rule (2.11), we can show that a spider with two inputs and one output behaves like a classical XOR gate when applied to the eigenstates of the *same* basis. Whilst using the state copy rule (2.13), we can show that a spider with one input and two outputs behaves like a classical COPY gate when applied to the eigenstates of the *opposite* basis.

Figure 2.14: XOR gate (left) and COPY gate (right) with respect to the Z eigenstates.

Hence, using the natural commutation relation of the classical XOR and COPY gates, we define the *bialgebra* rule. We encourage the reader to verify this relation.
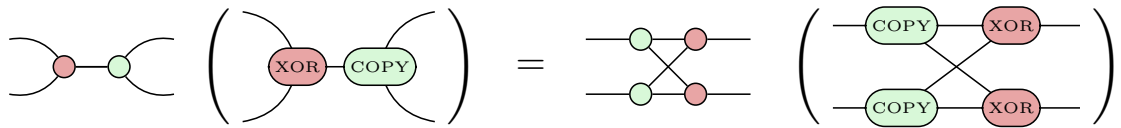
Chapter 3

Pauli Gadgets

Pauli gadgets form the building blocks for ansätze for quantum chemical simulations. We will see in Chapter 5 how they can be used to construct excitation operators in Unitary Product State ansätze.

A Pauli string P is defined as a tensor product of Pauli matrices $P \in \{I, Y, Z, X\}^{\otimes n}$, where n is the number of qubits in the system. Each Pauli gate acts on a distinct qubit. Thus $Z \otimes X$ represents the Pauli Z and X gates acting on the first and second qubits respectively.
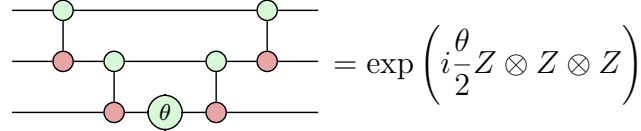
Stone's Theorem states that a strongly-continuous one parameter unitary group $U(\theta) = \exp(i\frac{\theta}{2}P)$ is generated by the Hermitian operator P [15]. Since the Pauli matrices, and consequently Pauli strings, are Hermitian, we can use the one-to-one correspondence between Hermitian operators and one parameter unitary groups to define Pauli gadgets as the one parameter unitary groups associated with a given Pauli string.

$$\Phi_1(\theta) = \exp\left(i\frac{\theta}{2}Z \otimes I \otimes Z\right) \qquad \Phi_2(\theta) = \exp\left(i\frac{\theta}{2}Y \otimes Z \otimes X\right)$$

Figure 3.1: Two example Pauli gadgets
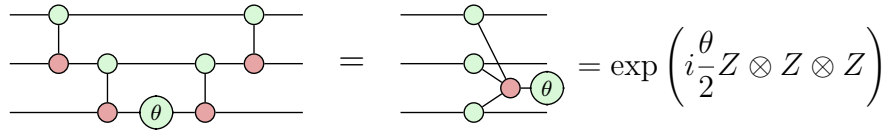
3.1   Phase Gadgets

Phase gadgets are defined as the one parameter unitary groups of Pauli strings consisting of the I and Z matrices, $P \in \{I, Z\}^{\otimes n}$. They correspond to quantum circuits made of a Z rotation sandwiched between two ladders of CNOT gates.

$$\text{(circuit diagram)} = \exp\left(i\frac{\theta}{2} Z \otimes Z \otimes Z\right)$$
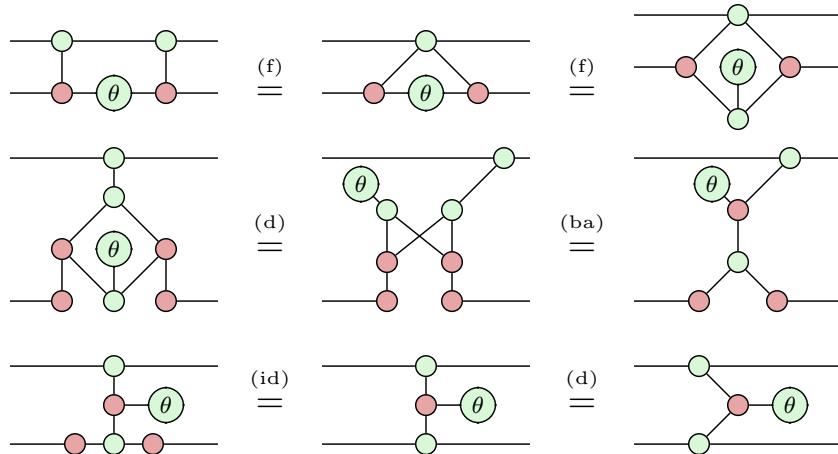
Phase gadgets necessarily correspond to diagonal unitary matrices in the Z basis, since they apply a global phase to a given state without changing the distribution of the observed state [2]. This diagonal action suggests that a symmetric ZX diagram exists for phase gadgets, as is indeed the case.

$$\text{(ZX diagram)} = \text{(ZX diagram)} = \exp\left(i\frac{\theta}{2} Z \otimes Z \otimes Z\right)$$

Phase gadgets can be interpreted as first copying each input in the Z basis (2.14), computing the parity of the state by taking the XOR (2.14), then multiplying the state by $\exp\left(-i\frac{\theta}{2}\right)$ or $\exp\left(i\frac{\theta}{2}\right)$ depending on the parity [2].

By deforming d our phase gadget in quantum circuit notation and using the identity id (2.12), spider fusion f (2.11) and bialgebra ba (2.2) rules, we are able to show the correspondence with its form in the ZX calculus.

3. Pauli Gadgets

It is then a simple matter of recursively applying this proof to phase gadgets in quantum circuit notation to generalise to arbitrary arity.
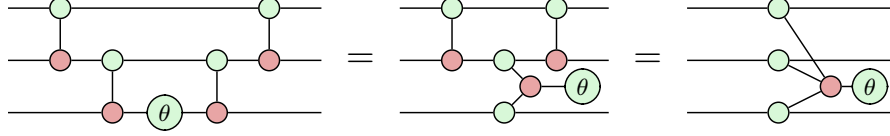
As well as being intuitively self-transpose, and hence diagonal, this representation comes equipped with various rules describing the interactions of phase gadgets.

Phase Gadget Identity

Phase gadgets with an angle $\theta = 0$ can be shown to be equivalent to identity using the state copy (2.13), spider fusion (2.11) and identity removal (2.12) rules.
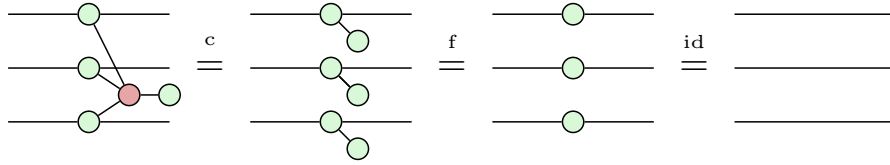
Phase Gadget Fusion

Any two adjacent phase gadgets formed from the same Pauli string fuse and their phases add. This is achieved using the spider fusion rule (2.11) and the bialgebra rule (2.2). See Appendix 7.2 for the intermediate steps marked (*).
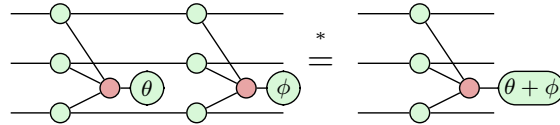
Phase Gadget Commutation

We can show that adjacent phase gadgets commute using spider fusion (2.11).
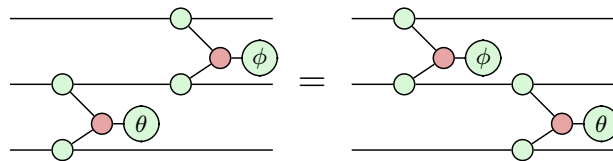
Phase Gadget Decomposition

SHOW THE DIFFERENT WAYS OF DECOMPOSING A PHASE GADGET AS EITHER UP OR DOWN.

There are many equivalent ways of decomposing a phase gadget into quantum circuit notation using the bialgebra rule (2.2). More generally, we can show that it is possible to decompose a phase gadget such that it his a circuit depth of $\log_2(n)$ instead of n, where n is the number of qubits.
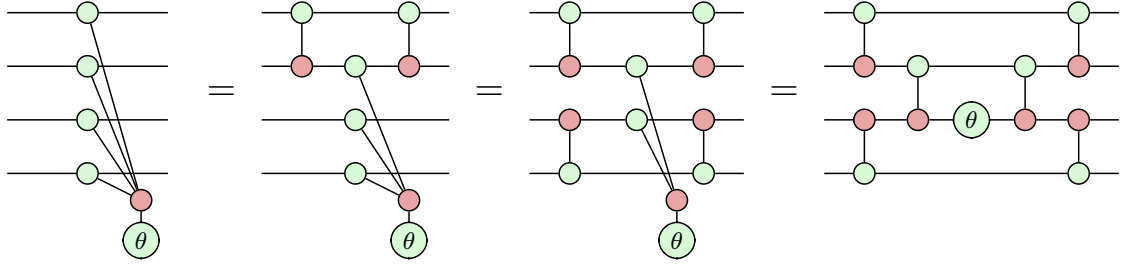
Phase gadgets can be thought of as the many-qubit generalisation of Z rotations [2]. To show this, let us consider a single-legged phase gadget. Using the bialgebra (2.2), spider fusion (2.11), state copy (2.13) and identity (2.12) rules, we can demonstrate its equivalence to a Z rotation.
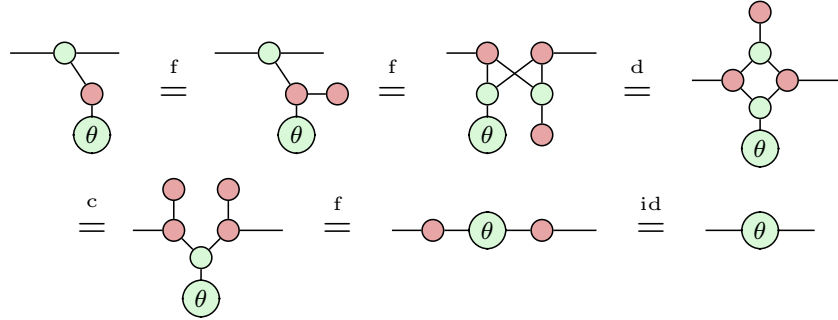
3.2 Pauli Gadgets

Pauli gadgets are defined as the one parameter unitary groups of Pauli strings consisting of all four Pauli matrices, $P \in \{I, Z, X, Y\}^{\otimes n}$ [2]. They are essentially phase gadgets with an additional change of basis.

$$= \exp\left(i\frac{\theta}{2}Y \otimes Z \otimes X\right)$$

Whilst phase gadgets alone cannot change the distribution of the observed state, Pauli gadgets are able to do so [2]. In chapter 5 we will see how Pauli gadgets form the building blocks in ansätze used for quantum chemical simulations.

Pauli gadgets come equipped with a similar set of rules to phase gadgets that describe their interactions with other gadgets. For instance, adjacent Pauli gadgets with *matching legs* fuse and their phases add modulo 2π.

Figure 3.2: Pauli gadget fusion rule

Similar to the phase gadget commutation rule (3.1), we have that adjacent Pauli gadgets with *no mismatching legs* commute.

Figure 3.3: Pauli gadget commutation rule

Single-legged Pauli gadgets correspond to rotations in their respective basis.

3.3   Commutation Relations

In this section we will develop a set of *commutation relations* describing the interaction of Pauli gadgets with the Clifford gates. Diagrammatically, we interpret this as what happens to a Pauli gadget when a Clifford is pushed through it.

The Clifford group is the set of transformations that normalise the Pauli group. Therefore, conjugating a Pauli string by a member of the Clifford group $C^\dagger P C$ is closed in the set of Pauli strings, $P \in \{I, X, Y, Z\}^{\otimes n}$, where n is the number of qubits the Clifford gate acts on. Similarly, conjugating a Pauli gadget $\Phi(\theta)$ by a member of the Clifford group always yields some other Pauli gadget $\Phi'(\theta) = C^\dagger \Phi(\theta) C$. For instance, when $C = \text{CNOT}_{1,2}$ and $\Phi(\theta) = \exp\left[i\frac{\theta}{2} Z \otimes Z \otimes Z\right]$, we can interpret the conjugation diagrammatically as the phase gadget decomposition result (3.1).

$$\Phi(\theta) \qquad\qquad \Phi'(\theta)$$
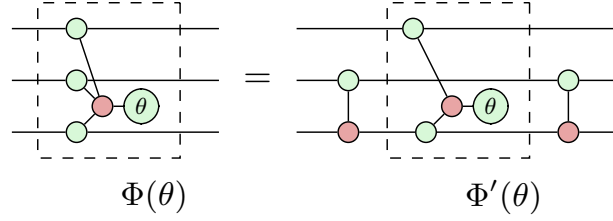
Recalling that the members of the Clifford group are unitary transformations, $C^{-1} = C^\dagger$, we can define *commutation relation* more formally as $\Phi(\theta)C = C\,\Phi'(\theta)$.

$$\Phi(\theta) \qquad\qquad \Phi'(\theta)$$
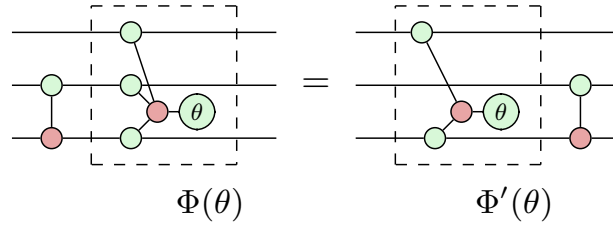
The CNOT gate is just one of many gates for which we can derive commutation relations. For example, consider the following Hadamard commutation relation.

$$\Phi(\theta) \qquad\qquad \Phi'(\theta)$$
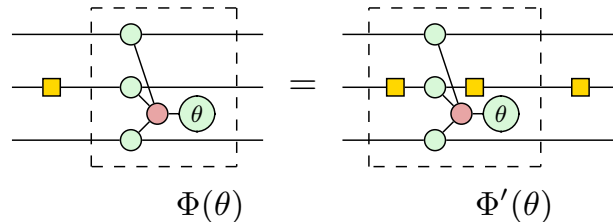
CNOT Commutation Relations

The CNOT gate acts on two qubits ($n = 2$), therefore, we can form 16 Pauli gadgets from Pauli strings of the set of Pauli matrices, $\{I, X, Y, Z\}$ taken two at a time, with repetition. In other words, there are 16 unique commutation relations to derive to fully describe the interaction between the CNOT gate and Pauli gadgets.
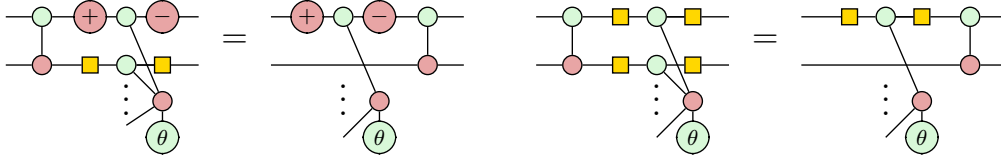

Figure 3.4: Two examples of the CNOT gate interacting with Pauli gadgets.

Whilst it is possible to derive each of these commutation relations using the Pauli gadget directly, it can be shown, through the Taylor expansion, that conjugating a Pauli gadget is equivalent to finding the one parameter unitary group of the conjugated Pauli string. Diagrammatically, this corresponds to pushing Pauli gates through some Clifford gate.

Let us illustrate the $\exp\left[i\frac{\theta}{2}Z \otimes Z\right]\mathrm{CNOT}_{0,1} = \mathrm{CNOT}_{0,1}\exp\left[i\frac{\theta}{2}I \otimes Z\right]$ commutation relation diagrammatically using the $Z \otimes Z$ Pauli string. We first push the bottom Pauli Z gate through the CNOT target using the π copy rule (2.13), then, we push the top Pauli Z gate through the CNOT control using the spider fusion rule (2.11), cancelling one of the copied Pauli Z gates in the process.
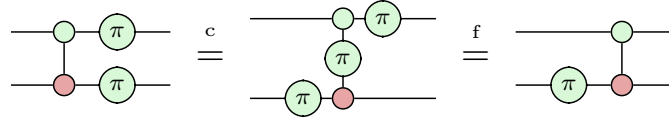
The Pauli Y gate can be expressed as a Pauli X gate followed by a Pauli Z gate, up to a global phase of $-i$ (CHECK). Below, we use this to illustrate the $\exp\left[i\frac{\theta}{2}Y \otimes X\right]\mathrm{CNOT}_{0,1} = \mathrm{CNOT}_{0,1}\exp\left[i\frac{\theta}{2}Y \otimes I\right]$ commutation relation.
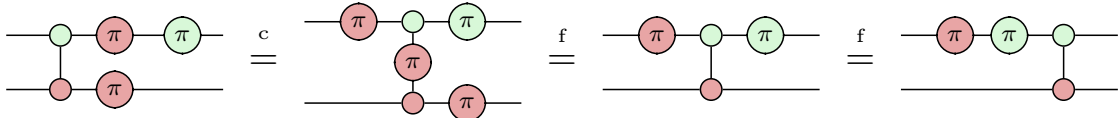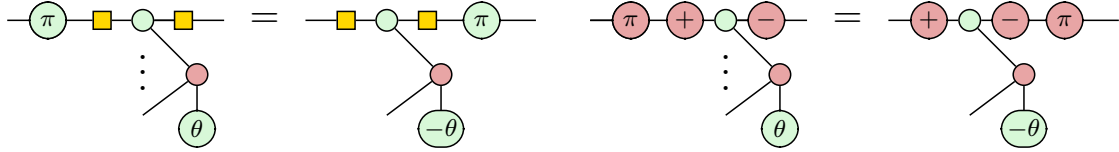
CZ Commutation Relations

Similarly, we can derive the 16 commutation relations of the CZ (controlled-Z) gate using the same method. Consider, for instance, the following example.
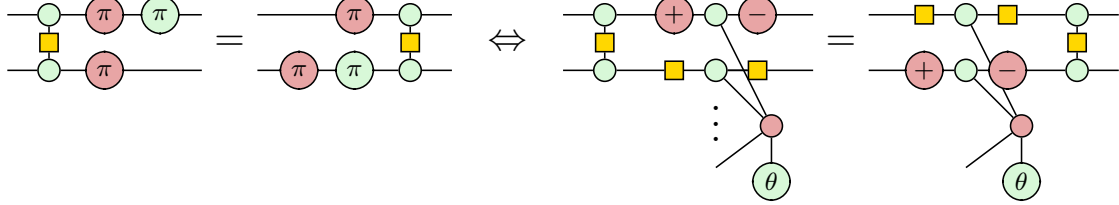
Pauli Commutation Relations

The Pauli matrices commute through Pauli strings by applying a global phase but leaving the Pauli string unchanged. Due to the one-to-one correspondence between Pauli strings and their corresponding Pauli gadget, we can show that the Paulis commute through Pauli gadgets by modifying their phase.

As pointed out by Richie Yeung, a more efficient method for identifying these commutation relations is instead to construct a Clifford tableau as in Winderl *et al* [16]. At the time, we were unaware of Clifford tableaus, however, using this method we were able to derive all 16 commutation relations (Appendix 2), demonstrating its efficacy. In Chapter 6, we choose to implement these commutation relations in our software package ZxFermion using Stim's (Clifford) `Tableau` class.

Chapter 4

Controlled Rotations

4.1 Singly Controlled-Rotations

In this section we will diagrammatically derive a singly-controlled rotation. A controlled rotation with respect to the Z eigenbasis applies a rotation to the target qubit if the control qubit is in the $|1\rangle$ state, and applies no rotation, if the control qubit is in the $|0\rangle$ state.

Let us start by considering the behaviour of the CNOT gate with the Z eigenstates. Using the state copy (2.13), we can show when the control qubit is $|0\rangle$, we obtain identity, whilst when $|1\rangle$ we obtain the Pauli X gate.
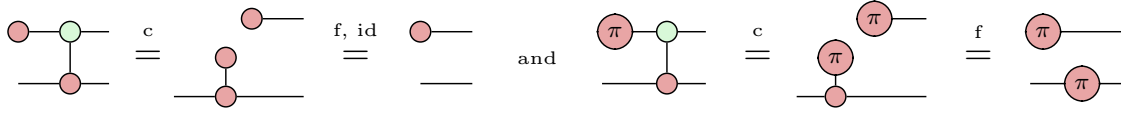
Next, using the π copy rule (2.13), we can show that conjugating a Z rotation by Pauli X gates, negates the phase of the rotation, $\alpha \to -\alpha$.
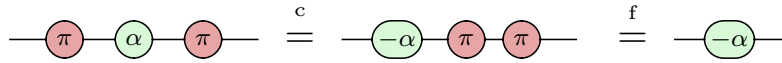
Combining these, we can construct a singly controlled rotation in the Z basis.
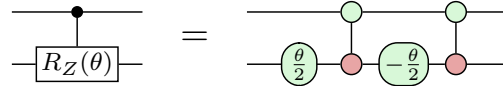
We can easily verify this by observing the behaviour of the Z eigenstates.
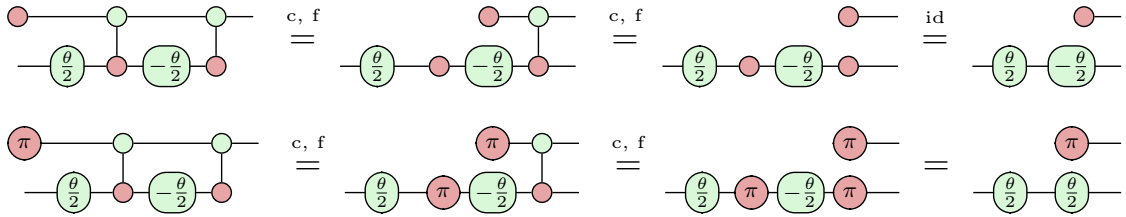
The resulting diagrams fuse to give identity or the Pauli X gate, as expected.

Using the bialgebra rule (2.2), we identify a two-legged phase gadget and a Z rotation.

4. Controlled Rotations
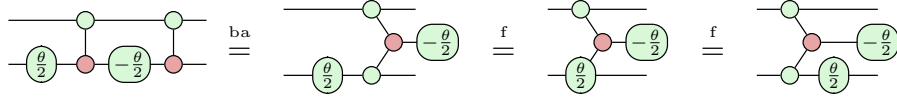
Using that the Z rotation commutes through the phase gadget (2.11), and the phase gadget decomposition rule (3.1) , we obtain four equivalent diagrams.
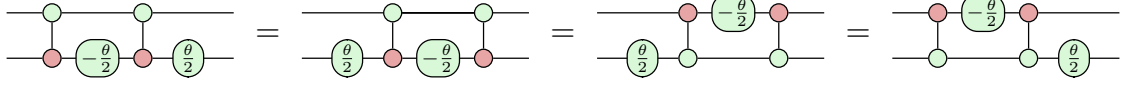
Deriving singly-controlled rotations in the X and Y bases amounts to conjugating the target qubit by the correct gates.
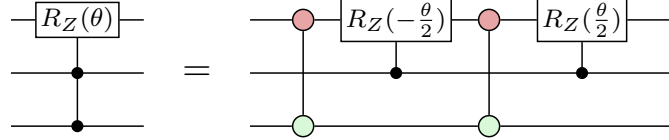

**Figure 4.1:** Singly-controlled X (left) and Y (right) rotations.

4.2 Higher Order Controlled-Rotations

We can implement higher order controlled rotations by nesting singly-controlled rotations in CNOT gates as in Yordanov *et al* [17]. For instance, we implement a doubly-controlled Z rotation as follows.


By representing the singly-controlled Z rotations in phase gadget form, we have the following.
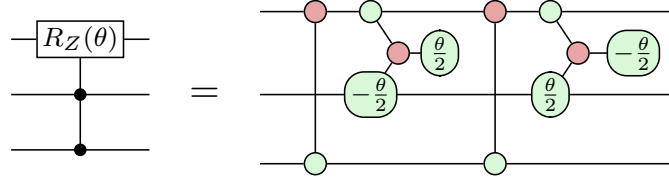
By decomposing each singly-controlled rotation into quantum circuit notation, we get the following. By carefully choosing how we decompose the singly controlled rotations, we can cancel one pair of $\text{CNOT}_{1,0}$ gates.
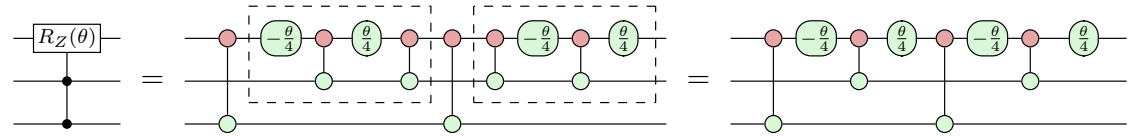
Using the commutation relations derived in Section 3.3, we can express the doubly-controlled rotation as the following phase polynomial.
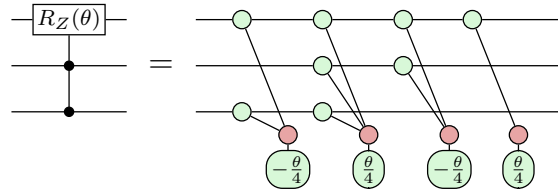
Chapter 5

Excitation Operators

Chapter 6

ZxFermion Software

ZxFermion (visit github.com/aymannel/zxfermion for documentation) is a Python package that I wrote for the manipulation and visualisation of circuits of Pauli gadgets. It is built on top of the PyZX `BaseGraph` API [18] and Stim [19]. The motivation for building this package came from the need for a user-friendly tool to explore research ideas related to circuits of Pauli gadgets.

Whilst there are existing software solutions like PauliOpt, which focus on circuit simplification using architecture-aware synthesis algorithms [20], ZxFermion provides a more acccessible alternative, as well as offering tools for studying the interaction of Pauli gadgets with Clifford and Pauli gates using Stim's `Tableau` class.

ZxFermion is designed to integrate with Jupyter notebook environments, enabling users to visualise interactive ZX diagrams directly in the output cell. The package has also undergone thorough testing, ensuring its reliability and ease of use.

All of the proofs so far derived can be replicated using ZxFermion, showcasing a noteworthy acceleration in research pace. We anticipate that both chemists and computer scientists exploring quantum computing within the VQE framework will find this software tool advantageous.

## 6.1   Creating Gadgets and Circuits

In this section, we will introduce the `Gadget` class, which we use to represent Pauli gadgets. We provide a Pauli string and a phase to instantiate a `Gadget()` object.

```
gadget = Gadget('YZX', phase=1/2)
gadget.draw()
```
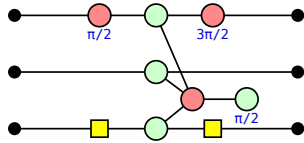

By setting the `as_gadget` option to `False`, we can view the gadget in its expanded form, that is, in quantum circuit notation.

```
gadget = Gadget('YZX', phase=1/2, as_gadget=False)
gadget.draw()
```
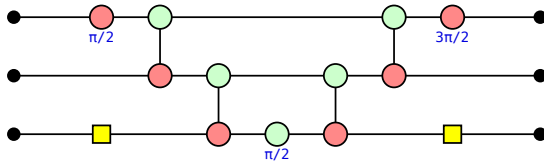

We can construct a circuit of Pauli gadgets using the `GadgetCircuit` class. The underlying data structure for this class is simply an ordered list.

```
gadget1 = Gadget('YZX', phase=1/2)
gadget2 = Gadget('XZY', phase=3/2)
circuit = GadgetCircuit([gadget1, gadget2])
circuit.draw()
```
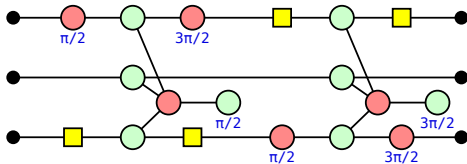

ZxFermion also implements standard quantum gates via the `CX`, `CZ`, `X`, `Z`, `XPlus`, `XMinus`, `ZPlus` and `ZMinus` classes. As we will see in the next section, we have implemented the logic describing the interaction of Pauli gadgets with these gates.

6.2 Manipulating Circuits

The `GadgetCircuit` class comes equipped with the `apply()` method that allows us to insert a quantum gate, and its Hermitian conjugate, into the circuit. This operation preserves the matrix corresponding to a given cricuit. The method takes the quantum gate to apply as its first parameter, whilst the `start` and `end` parameters designate the insertion positions.

```
gadget = Gadget('YZ', phase=1/2)
circuit = GadgetCircuit([gadget])
circuit.apply(CX(0, 1), start=0, end=0, draw=True)
```
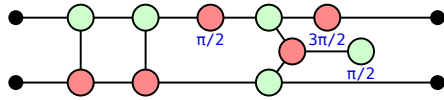

If no specific positions are specified, the insertion defaults to placing one quantum gate at the start, and its Hermitian conjugate at the end, of the circuit. The `GadgetCircuit` class then manages the relevant commutation relations, ensuring the expected gadget outcome. Hence, we below, we observe the gadget that results upon pushing a CNOT gate through the `Gadget("YZ", phase=1/2)` object.

```
circuit.apply(CX(0, 1), draw=True)
```
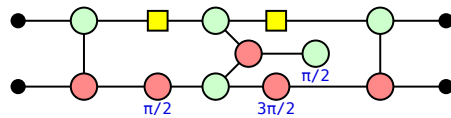

We could have chosen any Pauli gadget by simply instantiating the relevant `Gadget()` object. Alternatively, we could have chosen to insert any Hermitian conjugate pair of gates. The commutation logic implements Stim's `Tableau` class to identify the behaviour of a Pauli string with a given Clifford or Pauli gate.

```
circuit.apply(CZ(0, 1), draw=True)
```
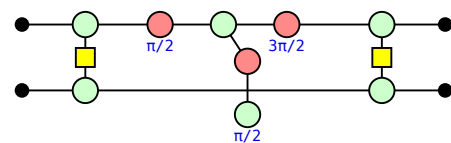
6. ZxFermion Software

The `GadgetCircuit` class offers the ability to manipulate circuits containing multiple gadgets simultaneously. Below, we instantiate the parametrised exponential of the single excitation operator, $a_0^\dagger a_1 - a_1^\dagger a_0$, in terms of quantum gates.

```
gadget1 = Gadget('YX', phase=1/2)
gadget2 = Gadget('XY', phase=3/2)
circuit = GadgetCircuit([gadget1, gadget2])
circuit.draw()
```
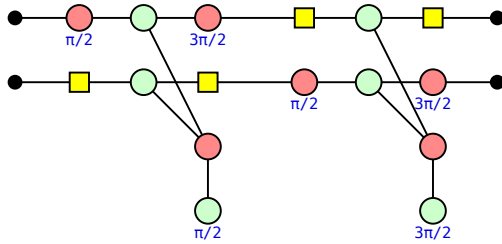

Conjugating the circuit with CNOTs reveals two Pauli gadgets, that combined, represent a controlled rotation in the Y basis. We have therefore faithfully replicated the result outlined in Yordanov *et al* [17].

```
cliff = CX(0, 1)
circuit.apply(cliff, draw=True)
```
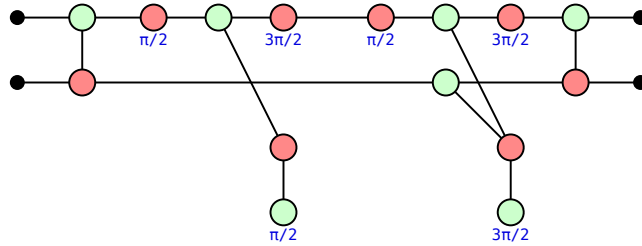

We consider it a significant achievement that with just a few lines of code, a user can now faithfully replicate derivations that took us many hours.

GIVE SOME MORE EXAMPLES IN COMPACT FORM INCLUDING CONJU-GATING BY XPLUS ETC

Chapter 7

Conclusion

7.1 Conclusion

7.2 Future Work

Appendices

Hadamard

Below are several equivalent definitions of the Hadamard generator. Note that the two rightmost definitions do not require any scalar correction.
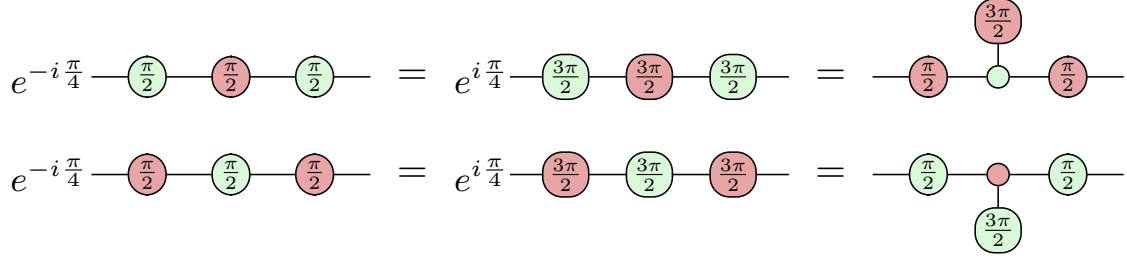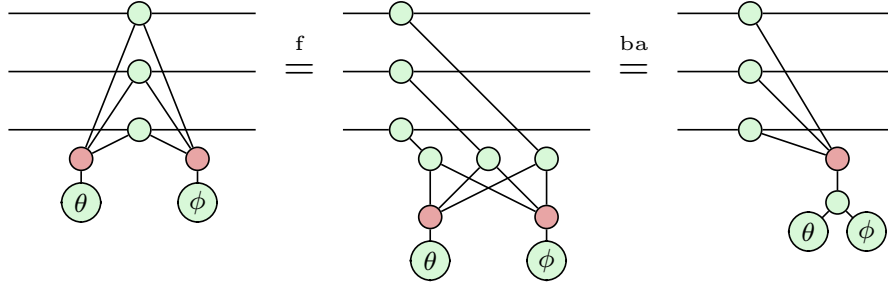

Figure 1: Equivalent definitions of the Hadamard generator.

Phase Gadgets

We can show how two adjacent phase gadgets fuse using the spider fusion (2.11) and bialgebra (2.2) rules as follows.

Clifford Conjugation Stuff

$$Ce^P C^\dagger = C \sum_{n=0}^{\infty} \left(\frac{P^n}{n!} \right) C^\dagger$$

$$CP^n C^\dagger = \sum_{n=0}^{\infty} \frac{CP^n C^\dagger}{n!}$$

$$CP^n C^\dagger = \sum_{n=0}^{\infty} \frac{(CPC^\dagger)^n}{n!}$$

$$CP^n C^\dagger = (CPC^\dagger)^n$$
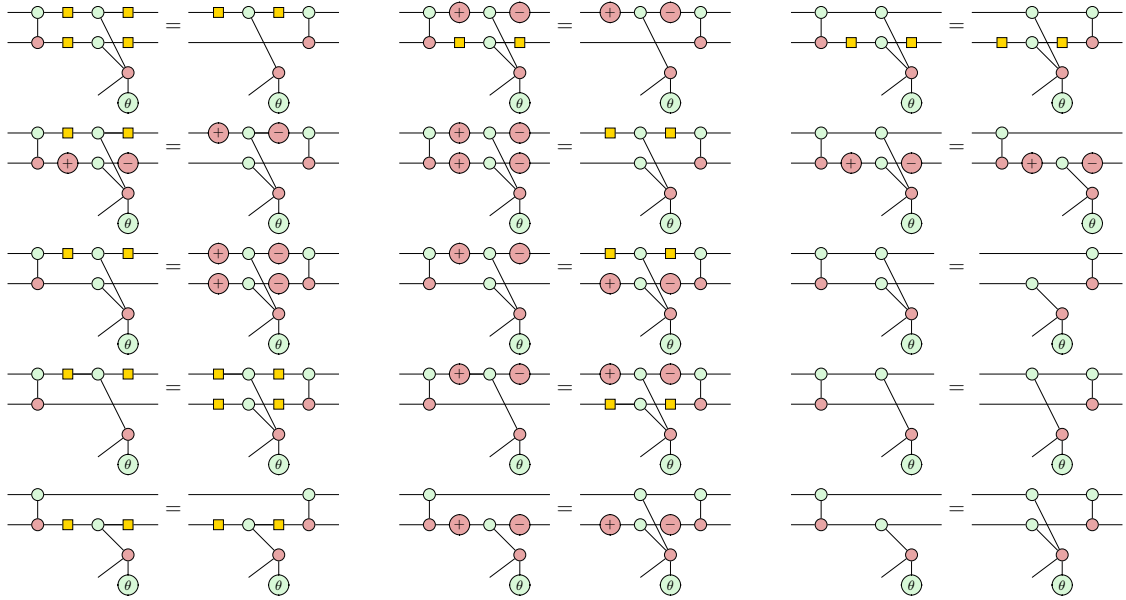
CNOT Commutation Relations

Figure 2: Complete set of CNOT commutation relations.

Bibliography

[1] Burton, H. G. A., Marti-Dafcik, D., Tew, D. P. & Wales, D. J. Exact electronic states with shallow quantum circuits from global optimisation. *npj Quantum Information* **9** (2023).

[2] Yeung, R. Diagrammatic design and study of ansätze for quantum machine learning (2020). `2011.11073`.

[3] McClean, J. R., Romero, J., Babbush, R. & Aspuru-Guzik, A. The theory of variational hybrid quantum-classical algorithms. *New Journal of Physics* **18**, 023023 (2016).

[4] Kirby, W. M. & Love, P. J. Variational quantum eigensolvers for sparse hamiltonians. *Phys. Rev. Lett. 127, 110503 (2021)* **127**, 110503 (2020). `2012.07171`.

[5] Nielsen, M. A. & Chuang, I. L. *Quantum Computation and Quantum Information: 10th Anniversary Edition* (Cambridge University Press, 2012).

[6] Szabó, A. v. & Ostlund, N. S. *Modern quantum chemistry : introduction to advanced electronic structure theory* (Mineola (N.Y.) : Dover publications, 1996). URL `http://lib.ugent.be/catalog/rug01:000906565`.

[7] Helgaker, T., Jørgensen, P. & Olsen, J. *Molecular Electronic-Structure Theory* (Wiley, 2000).

[8] Fetter, A. L., Walecka, J. D. & Kadanoff, L. P. *Quantum Theory of Many Particle Systems*, vol. 25 (AIP Publishing, 1972).

[9] Anand, A. *et al.* A quantum computing view on unitary coupled cluster theory. *Chemical Society Reviews* **51**, 1659–1684 (2021). `2109.15176`.

[10] Chan, H. H. S., Fitzpatrick, N., Segarra-Martí, J., Bearpark, M. J. & Tew, D. P. Molecular excited state calculations with adaptive wavefunctions on a quantum eigensolver emulation: reducing circuit depth and separating spin states. *Physical Chemistry Chemical Physics* **23**, 26438–26450 (2021).

[11] Seeley, J. T., Richard, M. J. & Love, P. J. The bravyi-kitaev transformation for quantum computation of electronic structure. *The Journal of Chemical Physics* **137** (2012). `1208.5986`.

[12] Peruzzo, A. *et al.* A variational eigenvalue solver on a photonic quantum processor. *Nature Communications* **5** (2014).

[13] Evangelista, F. A., Chan, G. K.-L. & Scuseria, G. E. Exact parameterization of fermionic wave functions via unitary coupled cluster theory. *The Journal of Chemical Physics* **151** (2019). `1910.10130`.

[14] van de Wetering, J. Zx-calculus for the working quantum computer scientist (2020). `2012.13966`.

[15] Stone, M. H. On one-parameter unitary groups in hilbert space. *The Annals of Mathematics* **33**, 643 (1932).

[16] Winderl, D., Huang, Q., de Griend, A. M.-v. & Yeung, R. Architecture-aware synthesis of stabilizer circuits from clifford tableaus (2023). `2309.08972`.

[17] Yordanov, Y. S., Arvidsson-Shukur, D. R. M. & Barnes, C. H. W. Efficient quantum circuits for quantum computational chemistry. *Physical Review A* **102**, 062612 (2020).

[18] Kissinger, A. & van de Wetering, J. Pyzx: Large scale automated diagrammatic reasoning. *Electronic Proceedings in Theoretical Computer Science* **318**, 229–241 (2020).

[19] Gidney, C. Stim: a fast stabilizer circuit simulator. *Quantum* **5**, 497 (2021).

[20] Gogioso, S. & Yeung, R. Annealing optimisation of mixed zx phase circuits. *Electronic Proceedings in Theoretical Computer Science* **394**, 415–431 (2023).